Reverse Engineering Prototype Solar PV/Thermal Collector Properties from Empirical Data for Use in TRNSYS Type 560

Nelson Sommerfeldt[1] and Patrik Ollas[2]

[1] KTH Royal Institute of Technology, Dept. of Energy Technology, Stockholm (Sweden)

[2] RISE Research Institutes of Sweden, Built Environment Division, Borås (Sweden)

Abstract

Using the known physical characteristics of a prototype photovoltaic-thermal (PVT) collector components and raw test data from a prematurely terminated ISO 9806 test, the objective of this study is to reverse engineer a thermal resistance value for the heat exchanger assembly for use in the theoretical TRNSYS model Type 560. Modeling is done using both TRNSYS as well as commercial heat transfer software TAITherm. Performance is measured by the mean absolute error and correlation of the outlet temperature and thermal power, as well as the differences in total thermal energy generated. The results show a thermal resistance of 0.005 to 0.010 m^2 K W^{-1} in TAITherm and 0.010 to 0.040 m^2 K W^{-1} in Type 560. TAITherm gives better statistical indicators which is likely due to the inclusion of thermal mass in the model. The results have informed prototype development and can be used in further systems modeling.

Keywords: PVT, Prototype, Testing, Simulation, TAITherm, TRNSYS, Validation

1. Introduction

Photovoltaic-thermal (PVT) hybrid modules absorb solar radiation and can convert it into electricity and heated fluids. There is a broad range of design concepts, however the most feasible solution for building applied or integrated products is a flat plate collector (Michael et al., 2015). In this arrangement, PV cells are mounted to a flat plate heat exchanger with cooling channels on the opposite side. With a glass front, this hybrid absorber can be used directly, known as an unglazed collector, or insulated from the environment with the glazing separated by an air gap over the PV. Insulation is most commonly added to the rear of the panel as well, but is not necessary.

PVT collectors are predominantly used for direct domestic hot water or space heating, and recently there has been growing interest in combining them with heat pumps (Hardorn, 2015). There are numerous potential system configurations, and one such configuration with relevance for Sweden is PVT in conjunction with ground source heat pumps (GSHP) (Sommerfeldt and Madani, 2016). If placed on the cold side of the heat pump, there are mutual benefits for each component; there is more energy captured from the solar collectors, the heat pump can receive a higher inlet temperature that improves the coefficient of performance (COP), and excess heat can be delivered to the borehole(s) for long-term storage.

A Swedish startup company is developing a system solution for integrating PVT collectors with GSHP. Unsatisfied with existing PVT products, they have decided to develop their own specifically designed for a GSHP application. Laminating PV cells directly to the absorber plate is difficult due

doi:10.18086/swc.2017.18.11 Available at http://proceedings.ises.org

to the need of a clean environment while also maintaining good electrical insulation between the absorber and PV cells (Zondag, 2008). PV manufacturing has matured to where the lamination process occurs with very high quality and low cost due to automation and economies of scale. This scale has yet to reach PVT collectors, which can be three to five times more expensive than a PV module due to the additional materials and complexity.

It is much simpler to take an off-the-shelf PV module and affix a heat exchanger to the rear side, either mechanically or with an adhesive. The greatest drawback of this approach is the reduced heat transfer between the PV cells and working fluid, thus reducing the electrical and thermal efficiencies (Zondag, 2008). However, if the cost of creating the heat exchanger can be substantially reduced, the loss of performance may be acceptable. This may be particularly so for PVT collectors in combination with heat pumps, where operating temperatures are much lower than most previous applications, thus removing the need for glazing and insulation due to lower losses (and potential gains) from the ambient air.

The Startup has gone through several prototype rounds tested in multiple installations, and has settled on a glass-glass PV module with an aluminum manifold mechanically pressed against the back. Using a glass backer allows greater contact with the heat exchanger and increases durability at the expense of increased thermal resistance. Opposite the PV module, the manifold has a trough to fit a 12 mm copper pipe, which is also mechanically fixed. Both interfaces are lined with thermal grease to encourage heat transfer. A cross section of the design is given in Figure 1 where it is compared with the models used in this study.

Two prototypes were tested according to ISO9806:2013 parameters during the autumn of 2016 at the RISE facility in Borås, Sweden with the goal of determining thermal performance coefficients of the empirical model described by Perers et al. (2012). However, issues with pressure drop and an unbalance flow were found late in the test cycle and were unable to be corrected before outdoor testing was forced to end for the winter. The result was a lack of data for making the necessary regressions, however there is enough raw data available to perform an empirical confirmation of theoretical models.

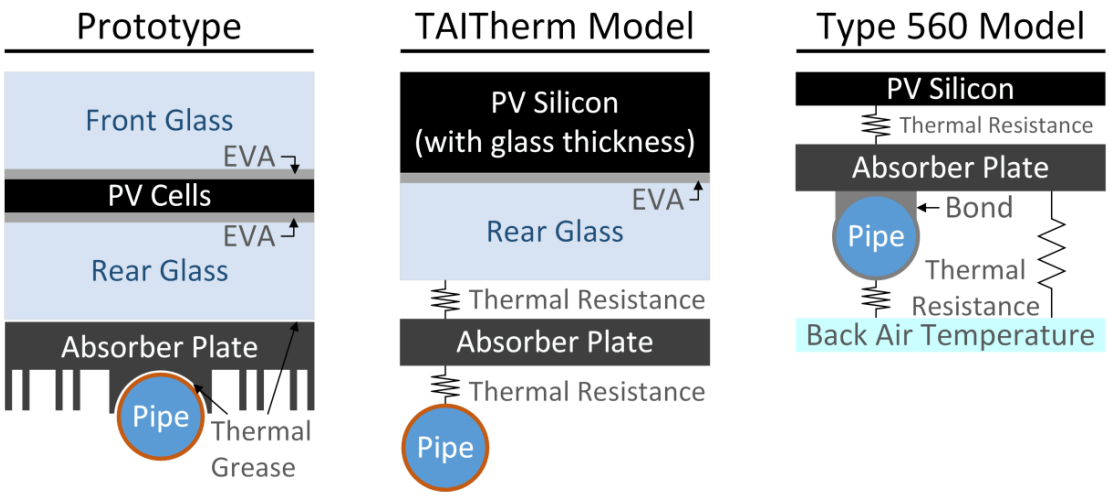

Figure 1 - Cross sectional representations of the PVT prototype, TAITherm, and Type 560 models (not to scale)

2. Objective and Methodology

With what is known about the PV module and heat exchanger construction, most of the collector's physical properties are fixed. The most critical missing characteristic is the conductive heat transfer behavior between the PV module and the pipes carrying the heat transfer fluid. Therefore, the primary objective is to determine a thermal resistance value between the PV module and the heat exchanger assembly to better understand the efficiency penalty of the design over dedicated PVT modules. This is done using the commercial heat transfer software TAITherm (ThermoAnalytics, 2016), which uses a numerical, finite volume approach. The motivation for using this modeling approach is twofold, 1) to capture the unconventional geometry of the heat exchanger, and 2) to independently control fluid streams for recreating the imbalanced flow observed during testing.

Collector development is just one part of a larger goal of PVT plus GSHP systems modeling, which is being done using the well-known tool TRNSYS (Klein et al., 2009). Therefore, the results from TAITherm need to be transferred into TRNSYS, which is most easily done using Type 560 whose theoretical model construction is most similar to TAITherm and the prototype. Given the differences between models, it is unlikely that the parameters will transfer directly, therefore the tuning process will be performed for TRNSYS as well. The results will also give a better understanding of the behavior of Type 560 which may be accounted for in systems models.

3. Method

Meeting the objectives involves a multistep process of constructing the model in TAITherm, manually tuning unknown parameters to achieve a best possible fit to empirical data, transfer of model settings into TRNSYS, and a manual re-tuning of parameters. The unknown parameters tuned with thermal resistance include; flow rates in each collector, absorptance and emittance of the PV module, and convection coefficients on the front and rear.

The mixed outlet temperature of the heat transfer fluid is used as the primary calibration measurement and thermal power used as a secondary indicator. In the TAITherm model, thermal power is calculated using the volumetric flow rate, fluid density, and inlet temperature measurements with modeled outlet temperature. In Type 560, thermal power is output directly from the model. Performance is measured using differences in total thermal energy generated as well as mean absolute error (MAE) and correlation of the outlet temperature and thermal power time series.

3.1 TAITherm Model Description

The TAITherm geometry is a 2.5 dimension mesh, meaning that the components are represented with surfaces and assigned multiple layers with individual properties. The PV module is represented by a 1.658 m by 0.992 m flat plate with 60 elements (10 x 6). The plate has three layers; the PV cells, plastic EVA encapsulate, and the rear glass as shown in Figure 1. A notable omission is the front glass layer. This is due to TAITherm's inability to model transparent and opaque layers together in a single part. The density of the glass and silicon are similar, so to adjust for the missing mass the thickness of the PV layer is made to encompass both the PV and glass. The layer thicknesses and material properties are given in Table 1. The primary sources for the physical characteristics of the module are the PV module spec sheet (Perlight PLM-260M) and from Armstrong and Hurley (2010).

Table 1 - Material properties of the TAITherm model

Layer	Material	Thickness	Density	Conductivity	Specific Heat
-	-	*mm*	*kg m⁻³*	*W m⁻¹ K⁻¹*	*J kg⁻¹ K⁻¹*
PV	Silicon	0.225 + 2.5	2330	148	677
EVA	EVA	0.5	960	0.7	2090
Rear Glass	Glass	2.5	2530	1.8	500
Tube	Copper	1	8954	390	383
Fluid	Water	-	Vary w/ temp	0.6	4186

The heat exchanger is represented by flat plat and a collection of six tubes, each a single layer part. As can be seen from the screen shot in Figure 2, the parts are not physically connected, but manually using a conduction link with a user input thermal resistance parameter. Both links are given the same thermal resistance since they are both mechanically pressed and have thermal grease between the parts. Inside the tubes are 1-D fluid streams that have convective heat transfer with a coefficient calculated using the pipe geometry, fluid velocity, and duct flow models incorporated into TAITherm. There are six pipes with corresponding fluid streams for each module, and the flow rates of each can be set independently. The streams all stem from a single fluid node and recombine into a single fluid node, which represent the measured inlet and outlet temperatures.

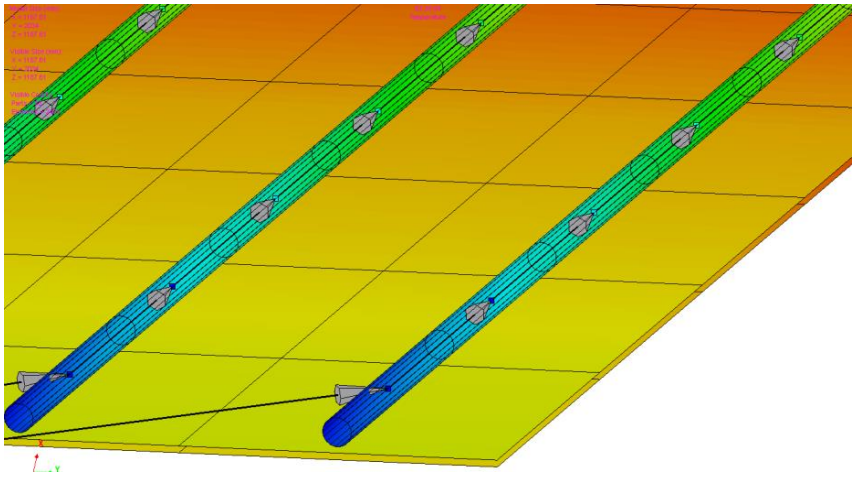

Figure 2 - Detailed view of the TAITherm model backside, showing the PV and heat exchanger parts

The internal heat transfer model within TAITherm is a dynamic, numerical solver based on first principle physics and has highly flexible inputs for boundary conditions. The measured irradiance is imposed directly on the front PV surface. PV generation is not modeled but instead the measured power is removed as heat from the back PV surface. Long wave infrared radiation was measured during testing and converted into sky temperature (T_s) using Equation 1 (Gliah et al., 2011), which is then used for radiant exchange. The collectors are mounted parallel with an asphalt roof within 15 cm, therefore the roof is the only rear view factor and is assumed to be the air temperature.

$$T_s = \left(\frac{Q_{lw}}{\sigma}\right)^{1/4} \qquad \text{Eq. 1}$$

$Q_{lw} = Long\ wave\ infrared\ irradiance\ (W\ m^{-2})$
$\sigma = 5.670\ x10^{-8}\ W\ m^{-2}\ K^{-4}$ (Stefan-Boltzmann constant)

3.2 Type 560 Model Description

Type 560 is one of two PVT models available from TESS, the makers of TRNSYS, and is based on the Hottel and Whillier model, later modified by Florschuetz, and described by Duffie and Beckman (2013). A full derivation and description is also available in the TESS library documentation and therefore will only be briefly reviewed here. The thermal model is the same as a standard solar thermal collector with fin-and-tube construction as shown in Figure 1. The primary modification is that the glazing has been removed and a PV model has been added on top of the absorber plate. One improvement of Type 560 over previous models is the inclusion of a thermal barrier between the PV cells and the absorber plate, a notable point of inefficiency in a PVT collector (Zondag, 2008). The calculation comprises of a set of 10 analytical equations are that solved iteratively since the power output of the PV cells is dependent on their temperature, which is also a function of the thermal collector.

The geometry and model construction of Type 560 and the TAITherm model are similar in several ways; the front glass of the PV module has been omitted, the thermal resistance between the PV cells and absorber plate can be set directly, and dynamic convection coefficients can be applied to front and back surfaces and to the working fluid. Major differences in 560 include modeled PV generation, rear insulation by default (represented by a thermal resistance input), the conduction between the absorber plate and tubes is defined with conductivity rather than thermal resistance, and there is no consideration for the collector's thermal mass.

3.3 Testing Conditions

Testing was performed on two prototype collectors, plumbed in parallel, and mounted on a south-facing roof at a 45° slope. Data was collected between September 19th and October 6th, 2016 using a five-minute time step. Three distinct periods are used in this study and are chosen due to the variation in inlet temperatures and their relatively long, continuous duration. The nominal volumetric flow rate in all of the testing is 240 l/h, equivalent to 0.02 l/s-m^2.

Test One occurs on September 19th, which was a warm and partly cloudy day, using a 10°C target inlet temperature. There are 9.5 hours of data total between 10:11 and 19:46, and Figure 3 shows the ambient air temperature, calculated sky temperature, total irradiance (measured in the collector plane), and wind speed.

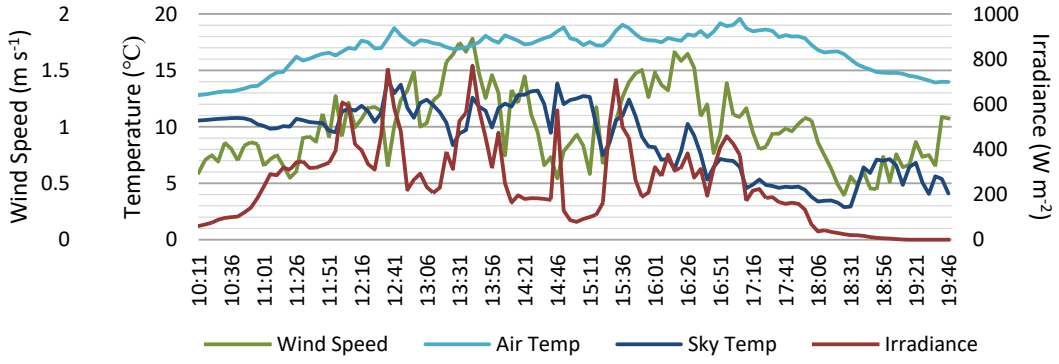

Figure 3 - Measured climate data for Test One

Test Two begins in the morning of October 5th and ends in the early afternoon on October 6th. During the mornings, there are some clouds but otherwise the skies are mostly clear with little wind as shown by the climate data in Figure 4. The inlet temperature target was 20°C, however the actual values are closer to 19°C.

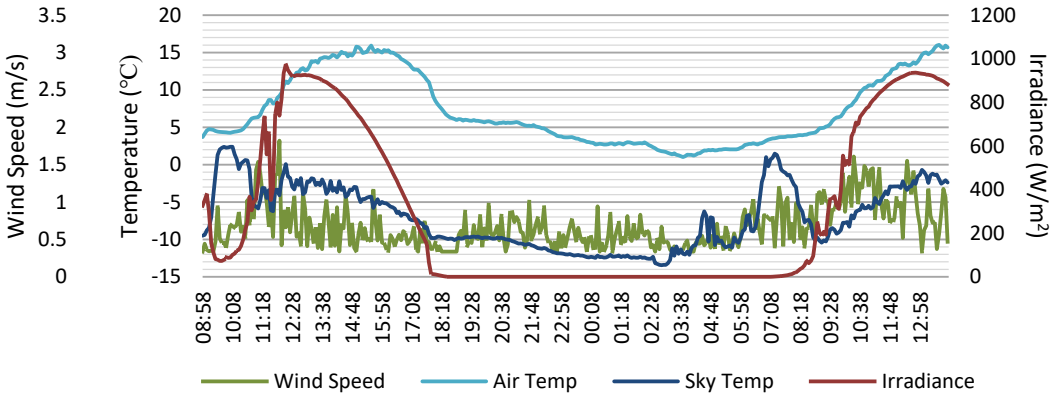

Figure 4 - Measured climate data for Test Two

Test Three is the longest at just over 46 hours, beginning the morning of September 24th and concluding in the morning of September 26th. During the majority of the test there were partly cloudy skies with little wind at night and a gentle breeze during the day, shown in Figure 5. The target inlet temperature here is 30°C, however most of the test has temperatures between 28°C and 29°C.

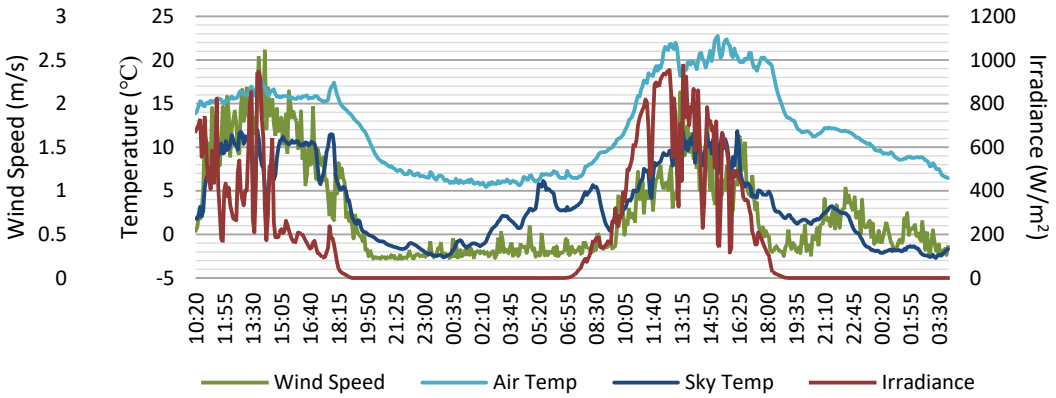

Figure 5 - Measured climate data for Test Three

4. Results

The first step in the tuning process is to determine the flow rates in each collector. An IR image taken during testing discovered the flow imbalance and is used here to compare with TAITherm results, shown in Figure 6. The post-processor in TAITherm allows the visualization of thermal gradients, however only the thermal patterns are considered and not the absolute temperature values. The image suggests that the majority of flow is through the right collector and several flow distributions (2%/98%, 1%/99%, 0%/100%) tested have determined that effectively all of the working fluid is passing through the right collector. Passing any significant amount of fluid through the left collector leads to a much less pronounced thermal gradient, however a negligible flow of 0.6 l/h is passed through the left collector for solver stability.

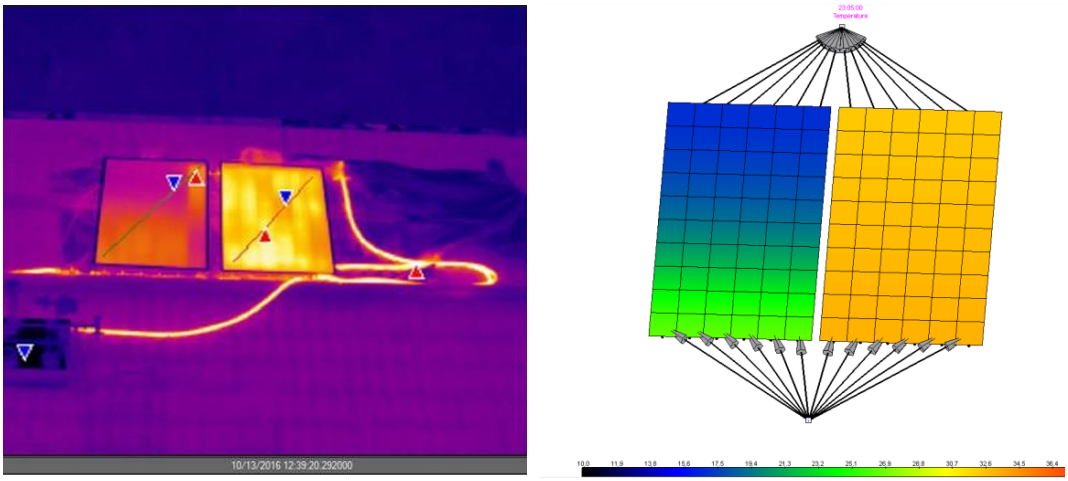

Figure 6 - IR image (left) during testing and TAITherm model (right) with 100% flow in the right collector

Convection on the front side is assumed to be wind dominated and several coefficient models have been tested, including; McAdams (1954), Test et al. (1981), and custom coefficients during the tuning process. Convection coefficients include a high degree of uncertainty (Mirsadeghi et al., 2013), and wind direction was not measured during testing which limits the ability to adjust the model for specific conditions. The commonly used McAdams model is found to be acceptable and is used on the front surface in all cases. The rear side of the collector was tested with both variable and constant convection coefficient models. All external convective heat transfer is modeled with the ambient air temperature.

Time series results are presented for each test in the following sections, while Table 2 with the statistical indicator results for all tests is given at the end of the section. Other common parameters include absorptance and emittance, which is found to be acceptable in all models at 0.85 and 0.90, respectively. It should also be noted that the range of plausible bond conductivities had an insignificant effect on the results for Type 560, meaning the primary tuning parameters are limited to the resistance between PV cells and absorber plate, rear convection coefficient, and the working fluid coefficient.

4.1 Test One

The thermal resistance discovered in TAITherm for Test One is 0.005 m^2 K W^{-1}, which applies to both the PV-absorber and absorber-tube interfaces. In Type 560, a resistance of 0.015 m^2 K W^{-1} is found to be a better fit. This only applies to the PV-absorber interface but includes the EVA and glass not included in the TAITherm value. The McAdams convection model is also an improvement for Type 560 where a fixed convection coefficient of 5 W m^{-2} K^{-1} is more suitable in TAITherm.

The time series results for temperature and power (both thermal and electric) are shown in Figure 7 and Figure 8, respectively. In these figures, it can be seen that the TAITherm model tracks the measured data more consistently than Type 560, with less pronounced peaks and valleys during strong irradiation events. This is confirmed with the performance indicators given in Table 2, where the TAITherm model is shown to have a lower MAE and higher correlation.

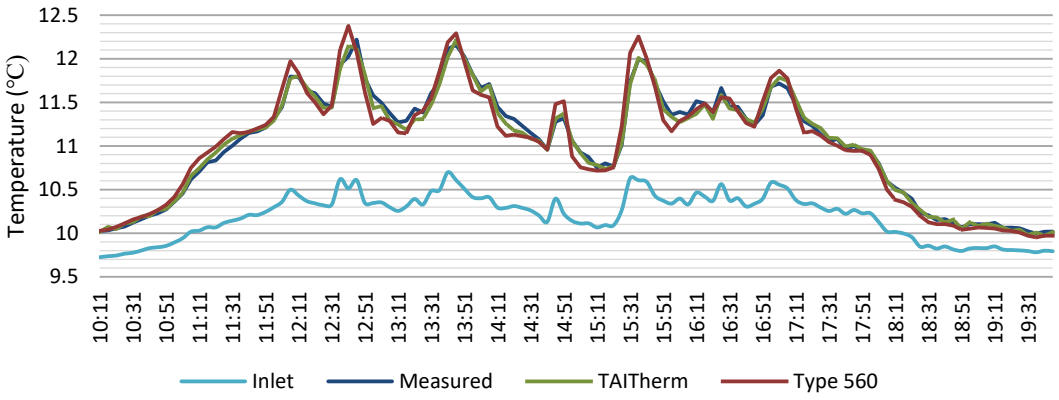

Figure 7 - Measured and model fluid outlet temperatures for Test One

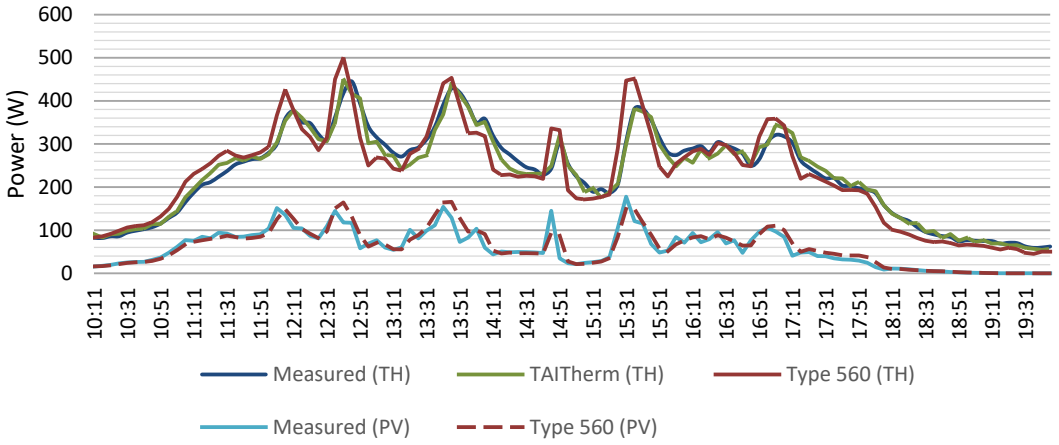

Figure 8 - Thermal and electrical power results for Test One

4.2 Test Two

The thermal resistance in Test Two for TAITherm is again 0.005 m^2 K W^{-1} while in Type 560 0.010 m^2 K W^{-1} is found to be a better fit. Once again the McAdams convection model is an improvement for Type 560 while a fixed coefficient of 5 W m^{-2} K^{-1} works better in TAITherm. The time series results shown in Figure 9 and Figure 10 show that Type 560 is tracking the measured data more closely when the irradiance is steadier with the clear skies. The performance indicators in Table 2 show a worse performance for TAITherm but approximately the same for Type 560 as in Test One.

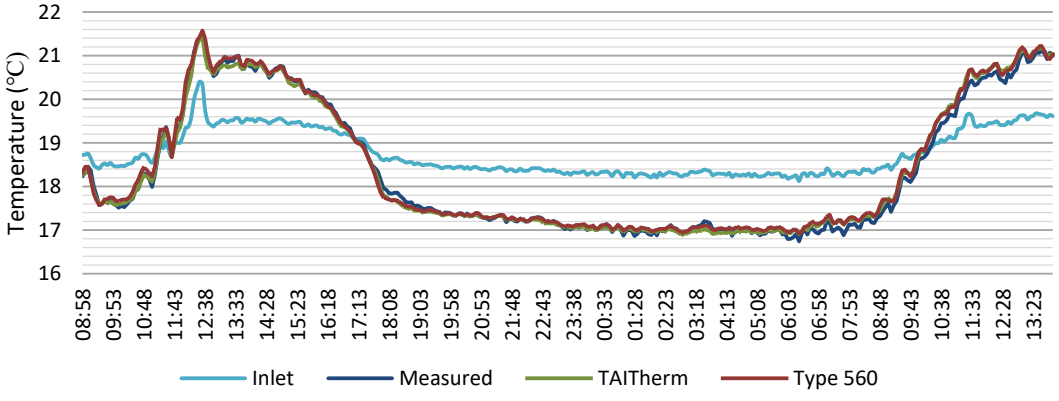

Figure 9 - Measured and model fluid outlet temperatures for Test Two

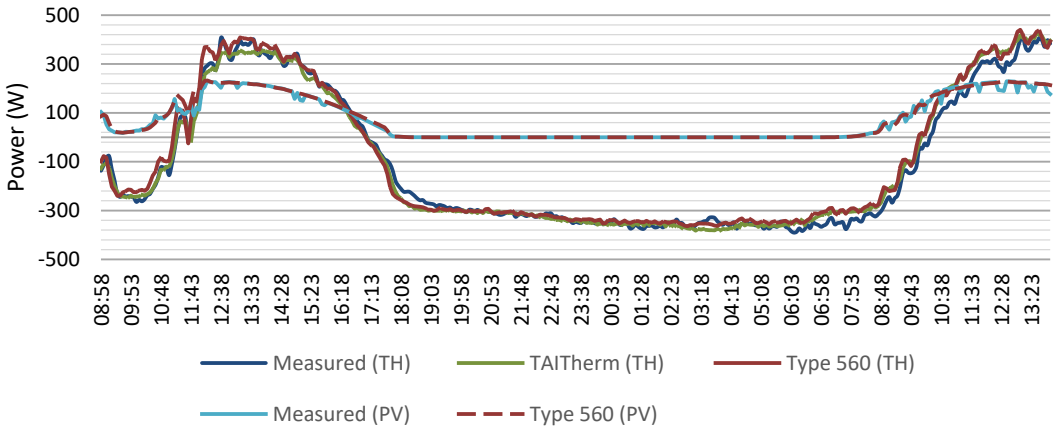

Figure 10 - Thermal and electrical power results for Test Two

4.2 Test Three

The thermal resistance in Test Three for TAITherm is increased to 0.010 m^2 K W^{-1} and 0.040 m^2 K W^{-1} for Type 560. In this test a static rear convection coefficient is best for both models and is the same in each at 6 W m^{-2} K^{-1}. The time series results shown in Figure 11 and Figure 12 are more difficult to interpret due to the longer timespan, however fluctuating irradiance again leads to a lower correlation for Type 560 during the daytime. The statistical indicators are notably worse for both models for this test as compared to the others.

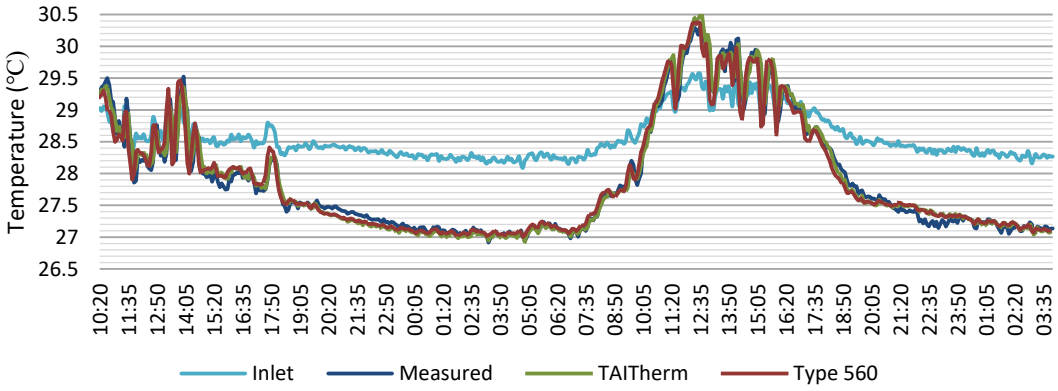

Figure 11 - Measured and model fluid outlet temperatures for Test Two

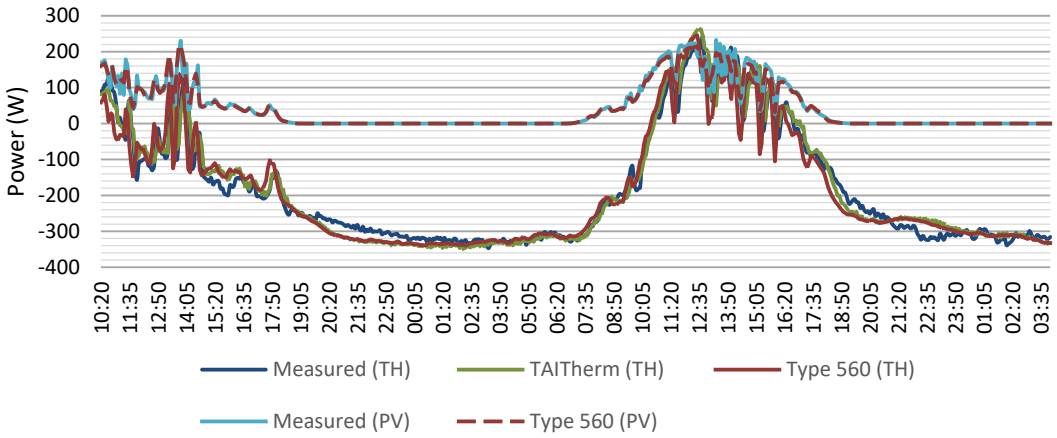

Figure 12 - Thermal and electrical power results for Test Two

Table 2 - Statistical performance indicators for all tests

Thermal Generation	Test One			Test Two			Test Three		
	Meas.	TAI	560	Meas.	TAI	560	Meas.	TAI	560
Total (kWh)	2.24	2.22	2.21	-3.24	-3.12	-2.74	-7.55	-7.52	-7.73
Diff. (kWh)	-	-0.02	-0.03	-	0.12	0.50	-	0.02	-0.19
Diff. (%)	-	-1.06%	-1.40%	-	-3.66%	-15.4%	-	-0.30%	2.46%

Electric Generation	Test One			Test Two			Test Three		
	Meas.	TAI	560	Meas.	TAI	560	Meas.	TAI	560
Total (kWh)	0.56	N/A	0.59	2.05	N/A	2.13	1.85	N/A	1.83
Diff. (kWh)	-	N/A	0.03	-	N/A	0.08	-	N/A	-0.02
Diff. (%)	-	N/A	4.86%	-	N/A	3.97%	-	N/A	-1.12%

	Test One		Test Two		Test Three	
Temp (K)	TAI	560	TAI	560	TAI	560
MAE	0.041	0.093	0.084	0.093	0.071	0.122
Correlation	0.997	0.983	0.997	0.998	0.996	0.979
Power (W_{th})	TAI	560	TAI	560	TAI	560
MAE	11.31	29.35	21.30	27.35	11.31	30.37
Correlation	0.989	0.939	0.996	0.994	0.989	0.961
Power (W_{el})	TAI	560	TAI	560	TAI	560
MAE	-	8.93	-	5.27	-	5.03
Correlation	-	0.945	-	0.990	-	0.984

5. Discussion and Conclusion

The tuning process is slow and tedious, however here it has produced two well performing models. The absolute uncertainty of the temperature probes is 0.1 K, therefore it is encouraging that MAE values are consistently below this. Besides uncertainty, the errors that remain are likely due to variations in the convection coefficients. Without knowledge of wind direction, it is difficult to know air speeds underneath the collectors. This is an addtional challenge with this type of PVT collector since the lack of insulation on the rear results in more sensitive convection gains or losses. In an actual installation, it is common to have skirting around the array such that air is not likely to pass underneath, which suggests a fixed coefficient will be more useful in systems modeling. Nevertheless, within this study the errors remain acceptably small particularly when considering larger systems models and annual simulations.

TAITherm produces results that are consistently better than Type 560, which is likely due to the modeling of thermal mass. With its glass-glass construction and thick aluminum extrusions, the PVT collector is approximately 35 kg, which is enough to potentially slow the response time of the heat transfer to the working fluid. This is seen in the time series data where there are rapid fluctuations in irradiance. It also appears in the Test Two statistical results, which had the most steady outdoor conditions and Type 560 performed the best. Adding thermal mass with other TRNSYS models in the system (e.g. pipes) could be a method to slow the thermal response. It is worth noting that this issue largely applies to studies where short time steps are critical. The energy generation values are within acceptable tolerances such that daily, monthly, or annual production is likely to be

reliable. This study does not quality as a full validation, however, and making these claims with certainty will require additional testing of the models against other data sets.

The modeling performed in this study has been valuable for several reasons. First, the thermal resistance values, summarized in Table 3, help place the performance of the prototype within other designs and/or products. Chow describes the thermal resistance between the PV cells and absorbers as being perfect when equal to 0.0001 m^2 K W^{-1}, and defective at 0.040 m^2 K W^{-1} (Chow, 2003). In this context, the 0.010 to 0.015 m^2 K W^{-1} values found with Type 560 in the first two test is relatively good, however the significantly higher value in Test Three is a cause for concern. A sensitivity analysis of this input is worthwhile when doing annual systems modeling, and the results here now provide a plausible range of values.

Table 3 - Thermal resistance parameters for each test and model (in m^2 K W^{-1})

	Test One	Test Two	Test Three
TAITherm	0.005	0.005	0.010
Type 560	0.015	0.010	0.040

Secondly, most solar thermal collector studies use the quadratic efficiency model. Having a theoretical PVT model is beneficial in that new designs without known efficiency coefficients can be modeled within systems, but it is important to have appropriate characteristics. The comparison between TAITherm and TRNSYS is useful because it validates the tuning process by having a second, fundamentally different model with similar results and it highlights the impact of the model structure on input parameters and the particular behavior of Type 560.

6. Acknowledgement

This research is funded by the Swedish Energy Agency under the Effsys Expand program, project number 40936-1.

7. References

Armstrong, S., Hurley, W.G., 2010. A thermal model for photovoltaic panels under varying atmospheric conditions. Appl. Therm. Eng. 30, 1488–1495. doi:10.1016/j.applthermaleng.2010.03.012

Chow, T.T., 2003. Performance analysis of photovoltaic-thermal collector by explicit dynamic model. Sol. Energy 75, 143–152. doi:10.1016/j.solener.2003.07.001

Duffie, J.A., Beckman, W.A., 2013. Solar Engineering of Thermal Processes, Fourth. ed. John Wiley & Sons, Inc., Hoboken, NJ.

Gliah, O., Kruczek, B., Etemad, S.G., Thibault, J., 2011. The effective sky temperature: An enigmatic concept. Heat Mass Transf. 47, 1171–1180. doi:10.1007/s00231-011-0780-1

Hardorn, J.-C. (Editor), 2015. Solar and Heat Pump Systems for Residential Buildings, First. ed. Ernst & Sohn GmbH & Co., Berlin.

Klein, S., Beckman, W.A., Mitchell, J., Duffie, J.A., Freeman, T., 2009. TRNSYS 17, A Transient System Simulation Program.

McAdams, W.H., 1954. Heat Transmission, Third. ed. McGraw-Hill, New York.

Michael, J.J., Iniyan, S., Goic, R., 2015. Flat plate solar photovoltaic – thermal (PV / T) systems : A reference guide. Renew. Sustain. Energy Rev. 51, 62–88. doi:10.1016/j.rser.2015.06.022

Mirsadeghi, M., Cóstola, D., Blocken, B., Hensen, J.L.M., 2013. Review of external convective heat transfer coefficient models in building energy simulation programs: Implementation and uncertainty. Appl. Therm. Eng. 56, 134–151. doi:10.1016/j.applthermaleng.2013.03.003

Perers, B., Kovacs, P., Olsson, M., Persson, M., Pettersson, U., 2012. A tool for standardized collector performance calculations including PVT. Energy Procedia 30, 1354–1364. doi:10.1016/j.egypro.2012.11.149

Pressiani, M., 2016. Photovoltaic/thermal hybrid solar collectors: TRNSYS analysis and possible improvements. Politecnico Milano.

Sommerfeldt, N., Madani, H., 2016. Review of Solar PV/Thermal Plus Ground Source Heat Pump Systems for European Multi-Family Houses, in: 11th ISES Eurosun Conference. Palma de Mallorca, Spain.

Test, F.L., Lessmann, R.C., Johary, a., 1981. Heat Transfer During Wind Flow over Rectangular Bodies in the Natural Environment. J. Heat Transfer 103, 262. doi:10.1115/1.3244451

ThermoAnalytics, 2016. TAITherm [WWW Document]. URL http://www.thermoanalytics.com/products/taitherm

Zondag, H., 2008. Flat-plate PV-Thermal collectors and systems: A review. Renew. Sustain. Energy Rev. 12, 891–959. doi:10.1016/j.rser.2005.12.012